Journal of Histochemistry & Cytochemistry 2018, Vol. 66(1) 7–22

DOI: 10.1369/0022155417737975
journals.sagepub.com/home/jhc
SAGE

CCR7 Is Important for Mesangial Cell Physiology and Repair

Simone Wurm, Andreas Steege, Eva-Maria Rom-Jurek, Claudia R. van Roeyen, Armin Kurtz, Bernhard Banas, and Miriam C. Banas

Department of Nephrology (SW, AS, EMRJ, BB, MCB) and Department of Gynaecology and Obstetrics (EMRJ), University Hospital Regensburg, Regensburg, Germany; Division of Nephrology and Immunology, Rheinisch-Westfälische Technische Hochschule Aachen University, Aachen, Germany (CRR); and Institute of Physiology, University of Regensburg, Regensburg, Germany (AK)

Summary

The homeostatic chemokine receptor CCR7 serves as key molecule in lymphocyte homing into secondary lymphoid tissues. Previous experiments from our group identified CCR7 also to be expressed by human mesangial cells. Exposing cultured human mesangial cells to the receptor ligand CCL21 revealed a positive effect on these cells regarding proliferation, migration, and survival. In the present study, we localized CCR7 and CCL21 during murine nephrogenesis. Analyzing wild-type and CCR7 deficient ($CCR7^{-/-}$) mice, we observed a retarded glomerulogenesis during renal development and a significantly decreased mesangial cellularity in adult $CCR7^{-/-}$ mice, as a consequence of less mesangial cell proliferation between embryonic day E17.5 and week 5 postpartum. Cell proliferation assays and cell-wounding experiments confirmed reduced proliferative and migratory properties of mesangial cells cultured from $CCR7^{-/-}$ kidneys. To further emphasize the role of CCR7 as important factor for mesangial biology, we examined the chemokine receptor expression in rats after induction of a mesangioproliferative glomerulonephritis. Here, we demonstrated for the first time that extra- and intraglomerular mesangial cells that were CCR7-negative in control rats exhibited a strong CCR7 expression during the phase of mesangial repopulation and proliferation. (J Histochem Cytochem 66:7–22, 2018)

Keywords

anti-Thy1.1 glomerulonephritis, kidney development, mesangiolysis, podocytes

Introduction

Nephron development as a tightly controlled process occurs as a result of dichotomous subdivisions of the ureteric bud (UB) induced by the metanephrogenic mesenchym (MM). That, in turn, condensates to renal vesicles (RV), which further differentiate into comma-shaped bodies (CSB) and S-shaped bodies (SSB). The latter is characterized by a cleft, where podocytes develop[1–3] and endothelial cells (EC),[4] followed by mesangial cells (MCs), migrate in. With transition to the capillary loop stage (CLS), MCs form a core surrounded by a single capillary loop.[5] Premised on their competence to adhere to the glomerular basement membrane (GBM), MCs split this single capillary loop in several capillaries giving rise to the glomerular tuft.[6]

Chemokines (chemotactic cytokines) are classified into four subfamilies (CXC, CC, CX3C, and XC) and serve as key molecules in mediating immune cell migration. In the context of immune response, chemokines are rapidly up-regulated and recruit leukocytes to loci of inflammation.[7] Contrarily, homeostatic chemokines like CCL21 and its receptor CCR7 are constitutively expressed and direct naïve T lymphocytes[8]

Received for publication April 11, 2017; accepted September 28, 2017.

Corresponding Author:
Miriam C. Banas, Department of Nephrology, University Hospital Regensburg, Franz-Josef-Strauß-Allee 11, 93053 Regensburg, Germany.
E-mail: miriam.banas@ukr.de

and dendritic cells (DC)[9] in secondary lymphoid tissues, with the objective of T-cell activation.[10]

In recent years, more chemokine functions have been described in addition to leukocyte recruitment and immune homeostasis, for example, their role in angiogenesis.[11,12] In the renal context, alterations in chemokine expression were mainly described under inflammatory and pathophysiological conditions, for example, the release of CCL2 by proximal tubular cells after stimulation with IL-1α[13] or the increased CXCR3 expression by patients suffering from IgA nephropathy.[14]

A renal phenotype depending on a particular chemokine expression under physiological conditions has not been identified, yet. Nevertheless, previous studies in our group demonstrated a podocytary CCL21 and mesangial CCR7 expression, respectively, in healthy adult humans.[15] Additional cell culture experiments exhibited a positive effect on human MCs[16] stimulated with CCL21 regarding mesangial adhesion, migration, and proliferation as well as a reduced susceptibility to induced apoptosis. Notably, the first three aspects are based on the enhanced CCL21-mediated mesangial ability to reorganize their cytoskeleton.[15,17,18]

The purpose of this study was to reveal the expanded role of CCR7 and its ligand in mesangial physiology by means of our animal models. Therefore, we performed localization experiments on renal specimens from developing and adult wild-type (WT) mice as well as from rats treated with an anti-Thy1.1 antibody. Furthermore, we examined the effect of CCR7 deficiency on mesangial physiology in vivo and in vitro.

Materials and Methods

Mice

C57BL/6J and B6.129P2(C)-Ccr7^{tm1Rfor}/J (CCR7$^{-/-}$) mice were purchased from The Jackson Laboratory (Sacramento, CA). CCR7$^{-/-}$ animals (stock number 006621) were backcrossed to C57BL/6 mice for 8 generations before sale. CCR7$^{-/-}$ mice were generated by Forster and colleagues by replacing amino acids from Ser-139 to Asp-309 by a neomycin resistance gene.[10] All mice were bred and housed under standard conditions with 12 hr day-night cycle with free access to water and chow. For embryonic kidney explantation, female WT mice were mated temporally controlled. For kidney extraction from postpartal and adult male mice, animals were anesthetized before intracardiac perfusion with HBSS (Life Technologies; Carlsbad, CA). All animal procedures were performed in accordance with national regulations for care and use of animals. Organ harvesting is not subject to approval by an institutional or licensing committee.

Rat Model of Anti-Thy1.1 Mesangioproliferative Glomerulonephritis

Male Wistar rats were obtained from Charles River Laboratories (Wilmington, MA) and kept under standard conditions with 12 hr day-night cycle with free access to water and chow. After reaching a weight of 180 g, anti-Thy1.1 mesangioproliferative glomerulonephritis was induced by injection of 1 mg/kg anti-Thy1.1 monoclonal antibody (clone OX-7; European Collection of Animal Cell Cultures; Salisbury, England). Kidneys were removed at 4, 24, and 48 hr as well as 4 and 7 days after antibody injection. Rats treated with PBS served as control. All animal procedures were performed in accordance with national regulations for care and use of animals and were approved by the local government authorities (Landesamt für Natur, Umwelt und Verbraucherschutz Nordrhein-Westfalen; Düsseldorf, Germany).

Isolation and Characterization of Primary Mouse Mesangial Cells

Primary mouse mesangial cells (pMMCs) were isolated from male CCR7$^{-/-}$ and WT mice at the age of 10 and 20 weeks (10w or 20w WT or CCR7$^{-/-}$, respectively). Therefore, kidneys were explanted and passed through a series of stainless steel sieves with the following mesh sizes: 150 µm, 100 µm, 70 µm, 50 µm. Glomeruli were collected on the 100 µm, 70 µm, and 50 µm sieve and treated with 0,1 mg/ml collagenase IV (Biochrome; Cambridge, UK) at 37C for 30 min. Glomeruli were transferred into fibronectin coated culture flasks and cultured in pMMC medium (DMEM low glucose, GlutaMAX, Life Technologies) supplemented with 20% fetal calf serum (Sigma Aldrich; St. Louis, MO), 2 mM L-glutamine, 1 mM sodium pyruvate, 5 ml non-essential amino acids solution (100×), 50 ng/ml Amphotericin B, 100 U/ml penicillin, 100 g/ml streptomycin (all Life Technologies), 5 µg/ml insulin, and 5 µg/ml transferrin (both Sigma Aldrich) in an atmosphere of 5% CO_2/95% air. After reaching a confluence of 90%, subcultivation was carried out by accutase (Life Technologies) treatment for 10 min. All pMMCs exhibit the typical stellate morphology. Characterization by immunostaining showed that pMMCs were positive for smooth muscle alpha-actin (Epitopics Inc; CA) and platelet-derived growth factor receptor beta (PDGFR-β) (Monoclonal IgG, clone Y92; Abcam, Cambridge, UK) and negative for cytokeratin 18 (Life Technologies).

Histochemical, IHC, and Fluorescent IHC Analyses

Mouse and rat kidneys were fixed with 4% paraformaldehyde and formalin, respectively. Histochemical and IHC examinations were carried out on 3 µm thick paraffin sections prepared by standard techniques. Localization studies were performed with the following primary antibodies: CCL21 (Monoclonal IgG2B, clone 59106; R&D Systems Inc.; Minneapolis, MN), CCR7 (Polyclonal Ig; Aviva, Systems Biology LLG; San Diego, CA), PDGFR-β, and Ki-67 (Polyclonal whole IgG, Bethyl Laboratories, Inc.; Montgomery, TX). For detection, we used a pre-formed enzyme-streptavidin (Strep)-complex (HRP-Strep or alkaline phosphatase [AP]-Strep, both Vector Laboratories Inc.; Burlingame, CA) that attached to the biotinylated secondary antibody. To localize CCL21 and CCR7 (both AP-Strep), we applied nitro blue tetrazolium/5-bromo-4-chloro-3-indolyl-phosphate as chromogenic reporter while nuclear fast red served as counterstain. For immunofluorescence-based detection of CCR7, an Alexa 594-Strep-complex (Life Technologies) was used as fluorochrome. PDGFR-β and Ki-67 were detected employing 3,3′-diaminobenzidine (DAB)—and, in addition, 0.09% $NiCl_2$ for Ki-67—and hematoxylin or nuclear fast red, respectively, as counterstain. As negative controls, we performed staining in the absence of each of the primary antibodies.

Mesangial Cell Quantification by Single Cell Analysis

Histomorphometric analyses of embryonic and postpartal murine kidneys were carried out with H&E stained renal sections using a Zeiss Observer microscope and AxioVision software (both Zeiss; Jena, Germany). The widths of the nephrogenic zone and renal cortex were measured in a blinded manner as described elsewhere.[19] Glomerular size was determined using HistoQuest 3.0 software (TissueGnostics GmbH; Vienna, Austria).[20] Therefore, glomerular tuft areas were manually defined as "regions of interest" (ROI). Based on the respective pixel size, the glomerular size was calculated. For single cell analysis, renal sections were stained for the mesangial cell marker PDGFR-β[21,22] and hematoxylin. PDGFR-β positive cells exhibited a DAB-brown hue; cell nuclei were blue. In all, 20 glomeruli per kidney were photographed in a blinded manner using an Axiostar plus microscope and AxioVision Release 4.8.1 software (both Zeiss; Jena, Germany). Subsequent evaluation was conducted using HistoQuest 3.0 software (TissueGnostics GmbH; Vienna, Austria). Glomerular tuft areas were manually encircled and defined as ROI. Only cells within the ROI were included in the analysis. Based on the HistoQuest 3.0 software algorithm, blue-stained nuclei were determined as single cells. Thereby, the amount of glomerular cells could be assigned. Every identified cell being, in addition, brown-stained was recognized as a PDGFR-β positive cell, or rather a mesangial cell.[20] Hence, the number of glomerular mesangial cells was ascertained.

Sodium Dodecyl Sulfate Polyacrylamide Gel Electrophoresis (SDS-PAGE) and Immunoblotting

For Western Blot analysis, pMMCs were grown in a 6-well plate supplemented with pMMC medium until confluency. After washing once with PBS, cells were lysed in 200 µl RIPA buffer per well with additive 100× Halt Protease and Phosphates Inhibitor Cocktail (Thermo Fisher Scientific Inc.; Waltham, MA). A bicinchoninic assay was performed to determine the protein concentrations; 10 µg protein per sample were electrophoretically separated, transferred to nitrocellulose membranes, and immunoblotted with antibodies against CCR7 (Monoclonal IgG, clone Y59; Abcam, Cambridge, UK) and glyceraldehyde-3-phosphate dehydrogenase (GAPDH) (Monoclonal IgG, Cell Signaling Technologies; Danvers, USA). For signal detection through horseradish peroxidase (HRP)-conjugated secondary antibodies, we used the ChemiDoc Imaging System (Bio-Rad; Hercules, CA).

Quantitative PCR Analyses

Total RNA was extracted from pMMC by applying peqGOLD Total RNA Kit according to manufacturer`s instruction (VWR International GmbH; Erlangen, Germany) and reverse transcribed in cDNA. To examine differential gene expression, primers were designed using Primer3 software (for primer sequences, see Suppl. Table 1). Their specificity and efficiency between 90% and 110% was confirmed beforehand. All samples were run in triplicates applying the QuantiTect SYBR Green PCR Kit (Qiagen; Hilden, Germany) and normalized to the expression of peptidylpropyl isomerase B (cyclophilin B) using the ViiA 7 Real-Time PCR System (Thermo Fisher Scientific Inc.). Fold change in expression was calculated using the $2^{-\Delta\Delta Ct}$ method.

Proliferation Assay

Cell proliferation was assessed by colorimetric BrdU cell proliferation assay according to manufacturer's instructions (BioVision; Milpitas, CA). From each of the four pMMC types, 5000 cells per well were dispensed into a 96-well plate with pMMC medium and allowed to adhere for 16 hr. Cells were treated with fresh pMMC

medium supplemented with 10 µM BrdU for 1 hr. This BrdU ELISA was performed in technical triplicates for three times always with pMMCs originating from a new passage.

Cell Migration Assay

In all, 5×10^5 cells from each of the four pMMC types were seeded per well of a 6-well plate and allowed to adhere overnight. After reaching confluence, the monolayer was scraped off with a rubber policeman to generate a linear cell-free area. Cells were washed twice with PBS, and new pMMC medium was added. To guarantee documentation of the same region, the wells were marked across the disrupted area. At 0, 24, and 48 hr after wounding, phase-contrast images of the corresponding regions were taken, and the width of the gap was determined using the AxioObserver.Z1 microscope (Zeiss; Jena, Germany). Each experiment was repeated 3 times.

Statistics

Statistical analysis was performed using IBM SPSS Statistics Version 21. Normal distribution was ascertained by the Shapiro-Wilk test, followed by a parametric ANOVA. In case of variance homogeneity or heterogeneity, the post-hoc test of Tukey and Kramer or Games-Howell, respectively, was applied. Non-normally distributed data were analyzed by Kruskal-Wallis non-parametric ANOVA. Ordinal data were statistically compared with the use of chi-squared tests. Statistical difference was set at the 5% level of probability.

Results

Renal CCR7 and CCL21 Expression in C57BL/6J Mice

Localization of the chemokine receptor by IHC staining revealed a strong expression in embryonic and early postpartal nephrogenesis (Fig. 1A–D). CCR7-positive structures in metanephroi were mesenchymal stromal cells and cells surrounding the cap mesenchym at day 14.5 of embryonic development (E14.5) as well as CSBs at E17.5. In late embryonic and postpartal kidneys, CCR7 was detected on early MCs in the CLS. However, with progressing development, glomerular CCR7 protein expression decreased and nearly disappeared in adult murine kidneys so that only a very weak, but still detectable expression was observed in fully developed glomeruli. Its ligand CCL21

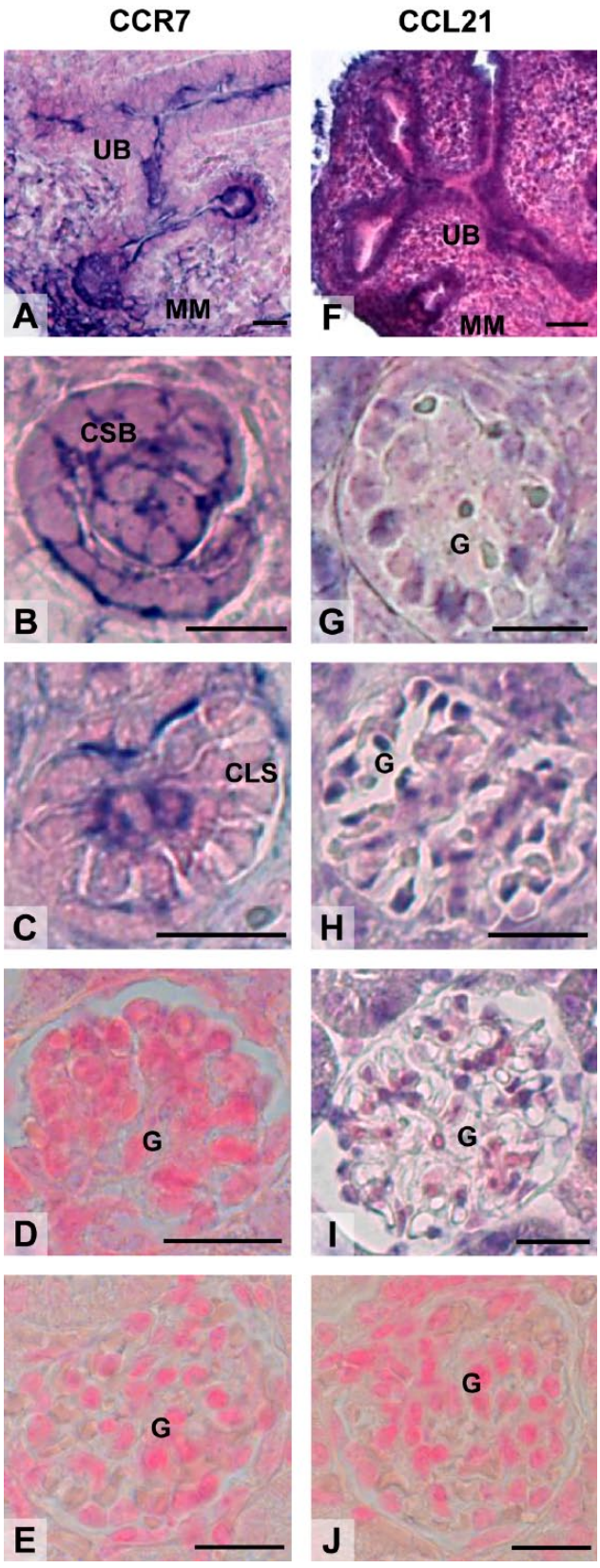

(continued)

Figure 1. Renal CCR7 and CCL21 expression in C57BL/6J mice. (A) CCR7 localizes within embryonic kidney at E14.5 on cells of the MM and in the UB and (B) in the CSB at E17.5. (C) Early glomerular MCs within the CLS at pp2 are positive for CCR7. (D) In mature glomeruli, CCR7 exhibits only a weak expression. (E) Negative control staining for CCR7. (F) CCL21 is expressed at E14.5 in the MM and in the UB. CCL21 shows a podocytary expression pattern (G) at E17.5 on early podocytes, (H) at pp2 on further developed podocytes, and (I) constitutively on differentiated podocytes in mature glomeruli. (J) Negative control staining for CCL21. CCR7 or CCL21 positive areas are blue, the counterstain is red. Scale bars: 20 μm; *n*=6–10. Abbreviations: MM, metanephrogenic mesenchym; UB, ureteric bud; CSB, comma-shaped body; MC, mesangial cells; CLS, capillary loop stage; G, glomerulus.

(Fig. 1F–I) was expressed in the MM and the UB during early embryonic nephrogenesis at E14.5. At this time, IHC localization of the chemokine ligand indicated an overall expression rather than a distinct expression pattern. With progressive glomerulogenesis, both early and further developed podocytes in embryonic or postpartal kidneys as well as fully differentiated podocytes in mature glomeruli were positive for CCL21.

Glomerular Development Is Delayed in Embryonic and Postpartal CCR7$^{-/-}$ Mice

Because the expression of CCR7 and its ligand CCL21 was detected to be most prominent during nephrogenesis, we subsequently investigated whether CCR7$^{-/-}$ deficiency already affects glomerulogenesis. As murine nephrogenesis is still incomplete at the time of birth, kidneys from WT and CCR7 deficient (CCR7$^{-/-}$) mice were examined at E17.5 and at day 2 and 5 postpartum (pp2, pp5) for the thickness of the nephrogenic zone (NZ). As the development of new nephrons was completed in both CCR7 WT and knockout animals at day 10 postpartum (pp10), here, the width of the renal cortex was measured. Additional analyses included counting the number of glomeruli normalized to the respective area, the mean glomerular size, as well as the glomerular cell number relative to the glomerular size, and the ratio of CLS bodies relative to further or fully developed glomeruli.

Regarding the width of NZ and the renal cortex, no difference was observed between age-matched WT and CCR7$^{-/-}$ animals in all groups (Fig. 2A and B). Subsequent quantification of the number of glomeruli revealed that age-matched WT and CCR7$^{-/-}$ kidneys contain approximately the same numbers of glomeruli (Fig. 2C). Next, we investigated the glomerular size. For E17.5 kidneys, whole sections were examined, whereas for pp2 and pp5 kidneys, the subnephrogenic zones, and for pp10 kidneys, subcapsular zones were analyzed. To examine only those glomeruli that have last developed, a 200 μm broad segment of the outer subnephrogenic zone or the outer periphery of the cortex was examined to prevent addressing also older, that is, fully developed, glomeruli in the inner cortex. Morphometric measurements demonstrated that postpartal CCR7$^{-/-}$ glomeruli are significantly smaller compared with WT glomeruli (Fig. 2D). The mean glomerular size of WT glomeruli from pp2 mice was 1194 μm^2 compared with 804 μm^2 in CCR7$^{-/-}$ animals. At pp5 or pp10, a mean glomerular size of 1222 μm^2 versus 895 μm^2 and 1078 μm^2 versus 687 μm^2 were measured. Although a trend was already recognizable, the size of E17.5 glomeruli did not significantly differ. To exclude that the reduced glomerular size observed in CCR7$^{-/-}$ animals was a result of smaller renal cells, the number of glomerular cells was also assessed and normalized to the size of the corresponding glomerulus. Our data revealed no differences between age-matched groups (Fig. 2E) indicating that a CCR7 deficiency did not have an effect on glomerular cell size or total number relative to the size of the glomerulus. Another reason for the reduced glomerular mean size was a potential developmental deficit. Therefore, the ratio of CLS bodies relative to further or fully developed glomeruli was determined. Our results demonstrated that in both genotypes, the number of CLS bodies declined with advancing age (Fig. 2F). Containing approximately the same amount of CLS bodies in E17.5 and pp2 kidneys, the ratio of CLS bodies decreased more pronouncedly in WT animals. With 27.5% versus 54.2% in pp10 kidneys, the difference between WT and CCR7$^{-/-}$ mice was statistically significant.

These data implicate that the glomerulogenesis of CCR7$^{-/-}$ rodents proceeds slower than in the WT pendant. The reduced glomerular size of CCR7$^{-/-}$ mice correlates with more glomeruli being in CLS, the stage of glomerulogenesis whose further development strongly depends both on the amount as well as on the proliferative and migratory capabilities of MCs.

CCR7 Deficiency Affects Mesangial Cellularity in Late Nephrogenesis and Adult Kidneys

Previous studies of our group suggested that CCR7 serves as proliferation and survival factor for MCs in vitro.[15,17,18] As we now could elucidate that the absence of the chemokine receptor impairs early glomerulogenesis in vivo, we subsequently aimed to analyze a possible correlation between a CCR7

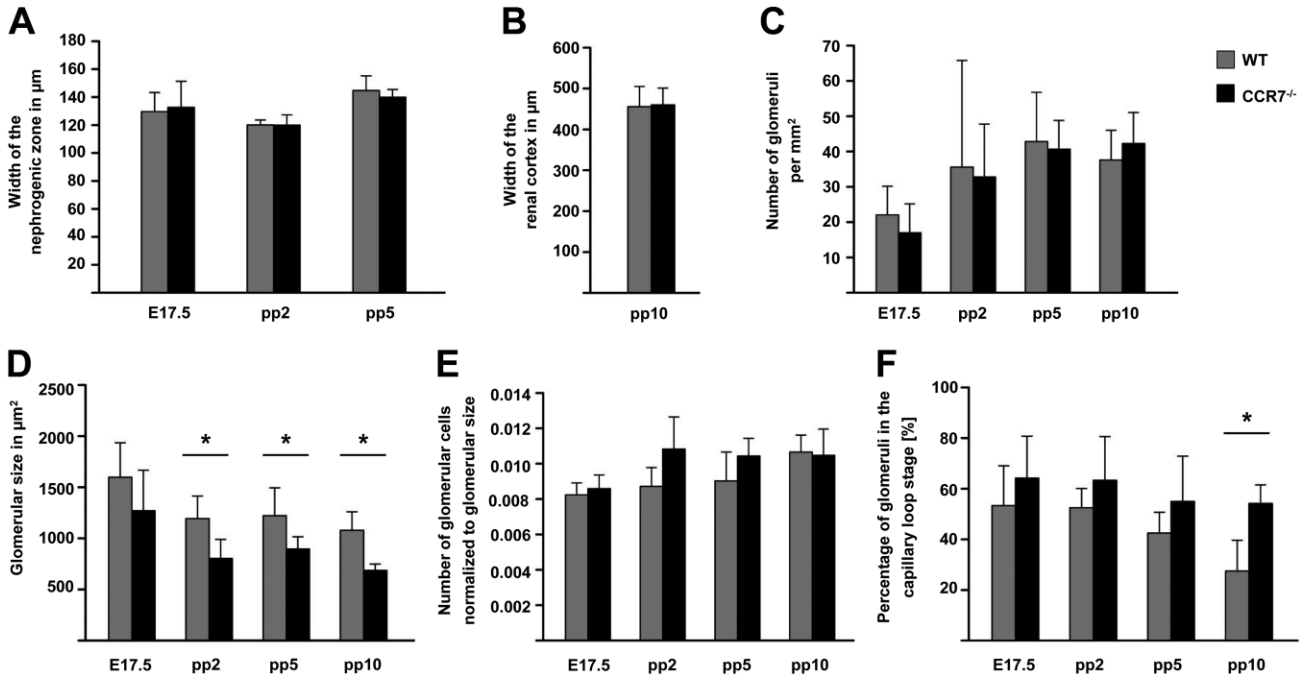

Figure 2. Histomorphometric analyses of embryonic and postpartal kidneys. (A) Width of the nephrogenic zone in kidneys from WT and CCR7$^{-/-}$ mice at embryonic day 17.5 (E17.5), day 2 (pp2), and day 5 (pp5) postpartum in µm. (B) Width of the renal cortex from WT and CCR7$^{-/-}$ mice at day 10 (pp10) postpartum in µm. (C) Number of glomeruli normalized to the analyzed area (mm^2) in embryonic (E17.5) and postpartal WT and CCR7$^{-/-}$ mice at pp2, pp5, and pp10. (D) Glomerular size in µm^2 in postpartal mice at E17.5 pp2, pp5, and pp10. (E) Quantification of glomerular cells relative to the size of the corresponding glomerulus in kidney from E17.5 pp2, pp5, and pp10 mice. (F) Ratio of glomeruli in the capillary loop stage in mice at E17.5 pp2, pp5, and pp10 relative to further developed or mature glomeruli. Gray bars represent mean data + *SD* for WT mice, black bars for CCR7$^{-/-}$ mice. Statistical analysis was conducted using one-way ANOVA. Abbreviation: WT, wild-type. *p<0.05 comparing age-matched groups; n=6.

deficiency and an altered mesangial cellularity in adult animals. We examined histological specimens from 5-, 10-, 15-, 20-, and 30-weeks-old male WT and CCR7$^{-/-}$ mice using the previously described mesangial cell marker PDGFR-β.[21,22] PDGFR-β was expressed in both genotypes (Supplemental Fig. 1), however, the staining intensity and extent exhibited interesting differences. With advancing age, only a slight decrease in staining was observable in WT animals. In contrast, CCR7$^{-/-}$ mice displayed a weaker staining intensity and extent.

Therefore, the next aim was to assess the number of intraglomerular (IG) MCs. Based on the PDGFR-β staining, we conducted a single cell analysis to quantify the number of both all glomerular cells and IG MCs (Supplemental Fig. 2). Our data show that CCR7 deficiency affects the number of MCs (Table 1). At the age of 5 weeks, CCR7$^{-/-}$ mice exhibited less MCs compared with age-matched WT animals regarding both the total and relative amount of MCs. For the first mentioned, statistical significance could be demonstrated (30 MCs in WT vs. 14 MCs in CCR7$^{-/-}$ mice). The absolute number of intraglomerular cells (IGC) was reduced as well (92 IGCs in WT vs. 81 IGCs in CCR7$^{-/-}$ mice). Therefore, we conclude that this was a result of diminished MC content because both genotypes exhibit comparable values regarding the remaining non-mesangial IGCs (64 IGCs in WT vs. 67 IGCs in CCR7$^{-/-}$ mice). Within the following 10 weeks, the amount of MCs decreased in WT animals and reached a stable level of approximately 14±1% from the age of 15 weeks. Contrarily, the MC number increased in CCR7$^{-/-}$ mice between the age of 5 and 10 weeks. Hereafter, the absolute and relative amount MC rapidly declined to a value of 9 in 15-weeks-old CCR7$^{-/-}$ mice. Having a relative cell content of 7%, 20- and 30-weeks-old CCR7$^{-/-}$ mice feature statistically significant less MCs compared with WT animals. Although the absolute IGC number significantly increased in 20- and 30-weeks-old CCR7$^{-/-}$ mice, a decline in total MC number was observed. One possible explanation for the increase of IGCs might be an influx of circulating immune cells into the glomeruli. To address this question, an additional IHC staining using a specific anti-MAC-2 antibody to stain infiltrating macrophages was performed. A statistically significant macrophage influx into glomeruli of 20- and 30-weeks-old CCR7$^{-/-}$ mice was detected (Supplemental Fig. 3).

Table 1. Intraglomerular Whole and Mesangial Cell Number.

	Total Glomerular Cell Number		Intraglomerular Mesangial Cell Number (Absolut)		Intraglomerular Mesangial Cell Number Relative to Total Glomerular Cell Number (%)	
Age	WT	CCR7$^{-/-}$	WT	CCR7$^{-/-}$	WT	CCR7$^{-/-}$
5 weeks	92 (88–104)	81 (78–90)	28 (21–32)	14* (12–19)	30 (23–33)	17 (15–27)
10 weeks	106 (100–113)	99 (96–109)	22 (19–24)	25 (19–29)	21 (18–22)	25 (18–32)
15 weeks	98 (91–104)	111 (106–118)	15 (10–16)	9 (8–22)	15 (12–16)	9 (7–20)
20 weeks	88 (82–96)	115* (108–120)	14 (11–16)	8 (6–10)	14 (9–21)	7* (4–11)
30 weeks	97 (94–99)	112* (105–116)	13 (11–14)	8* (6–12)	13 (8–18)	7* (4–13)

The total glomerular cell number, total intraglomerular mesangial cell number, and intraglomerular mesangial cell number relative to total glomerular cell number are presented as median with the interquartile range in parentheses. A total of 20 glomeruli per kidney were analyzed in a blinded manner. Medians were compared by non-parametric univariate ANOVA, followed by pairwise comparison using Kruskal-Wallis. *$p<0.05$ versus age-matched wild-type mice; $n=6–10$.

Retarded Development of the Glomerular Tuft in CCR7$^{-/-}$ Mice

Single cell analysis revealed a reduced MC number in 5-weeks-old CCR7$^{-/-}$ mice. Because MCs are essential for capillary tuft development, we analyzed glomerular developmental stages of 5- and 10-weeks-old mice of both genotypes based on the IHC staining against PDGFR-β. Thereby, glomeruli exhibiting a low or moderate number of MC-fields were evaluated with a score of 1 or 2, respectively. Mature glomeruli received a score of 3 (Fig. 3A). This analysis revealed that in 5-weeks-old WT animals, 63.3% of glomeruli were fully developed; 32.5% of glomeruli exhibited a moderate number of MC-fields and have, therefore, a partially built capillary convolute. Only 4.2% of examined glomeruli were identified to be in the CLS. Contrarily, in CCR7$^{-/-}$ mice, the percentage of mature glomeruli corresponded to only 34.2%. Thus, 49.2% of analyzed glomeruli featured a partially formed capillary tuft, and 16.6% were still in the phase of the CLS. However, this developmental deficit could be compensated until the age of 10 weeks, where no differences between the two genotypes were detected (Fig. 3B).

CCR7 Dependent Proliferative Properties of Glomerular MCs in vivo

To further characterize CCR7 dependent proliferation in vivo, histological sections from 5-, 10-, 15-, 20-, and 30-weeks-old WT and CCR7$^{-/-}$ mice were analyzed for the renal expression of the proliferation marker Ki-67 (Fig. 4A). Analyzing WT rodents, it could be seen that the quantity of proliferative cells decreased with advancing age in both glomeruli and tubules. Although an age-dependent decrease of renal cell proliferation was also seen for CCR7$^{-/-}$ mice, statistically significant differences compared with the WT were found in both the youngest and the oldest group (Fig. 4B). In the glomeruli of 5-weeks-old CCR7$^{-/-}$ mice, we detected 0.93 (±0.29) proliferating cells per glomerulus versus 0.48 (±0.07) in the age-matched WT group. In contrast, a reduced number of proliferating cells was seen in glomeruli in 30-weeks-old CCR7$^{-/-}$ mice.

Isolation of CCR7 Expressing Primary Murine Mesangial Cells

In the subsequent experiments, our goal was to further analyze the characteristics of glomerular MCs depending on their ability to express CCR7. Therefore, we isolated primary murine MCs (pMMCs) from 10- or 20-weeks-old WT animals and for subsequent in vitro studies also pMMCs from age-matched CCR7$^{-/-}$ mice.

The first aim was to demonstrate that 10w or 20w WT pMMCs express CCR7. Conducting qPCR experiments, we measured a C_T value of approximately 33 for CCR7, which represented an expression level close to the detection limit (data not shown). In addition, we prepared whole cell extracts and conducted an SDS-PAGE followed by Western Blot analysis. Our immunoblot (Fig. 5) against the chemokine receptor showed a single band of the predicted molecular weight of 43 kDa revealing that WT pMMCs express CCR7 on protein level independent from the age of mice the cells were isolated from. We could not detect the receptor in

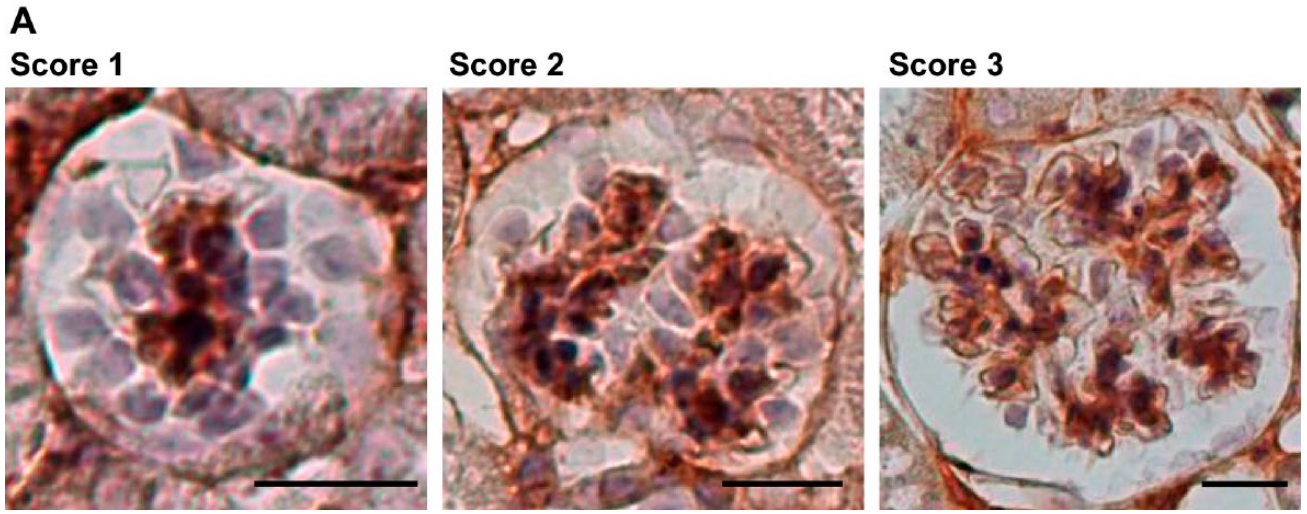

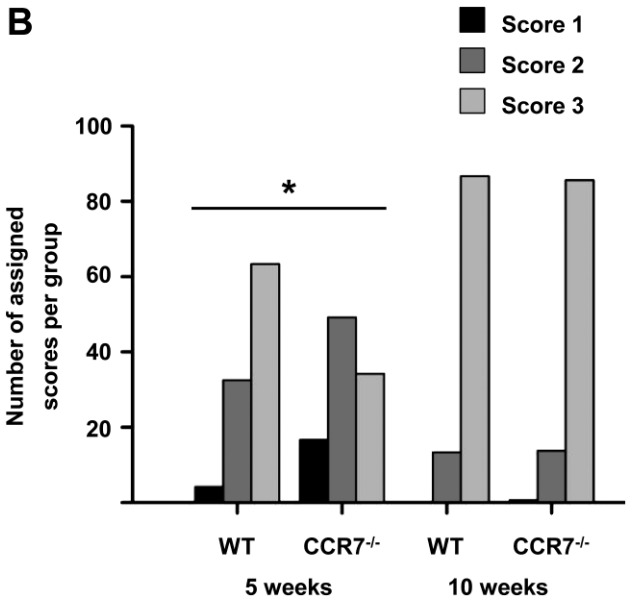

Figure 3. Development of glomerular tuft in 5- and 10-weeks-old WT and CCR7$^{-/-}$ mice. (A) Examples for PDGFR-β (brown) stained mesangia that illustrate allocated scores with corresponding developmental stages of glomerular convoluted capillaries. Score 1 represents a glomerulus in the capillary loop stage, score 2 an immature glomerulus with a few capillary loops, score 3 a mature glomerulus. Scale bars: 20 μm. (B) Number of assigned scores in 5- and 10-weeks-old WT and CCR7$^{-/-}$ mice regarding the development of the glomerular tuft. Statistical analysis was carried out by chi-square test. Abbreviation: WT, wild-type; PDGFR-β, platelet-derived growth factor receptor beta. *p<0.05 for age-matched groups; n=6–8.

pMMCs from CCR7$^{-/-}$ mice. A further blot to detect GAPDH served as loading control.

Differential Gene Expression in Primary Murine Mesangial Cells

To examine why WT and CCR7$^{-/-}$ mice exhibited different mesangial cellularities depending on age and genotype, we analyzed 10w or 20w WT or CCR7$^{-/-}$ pMMCs for their mRNA expression. We selected genes (Suppl. Table 2) that were described to control pro- and antiapoptotic processes as well as proliferation and migration in MCs.

We defined a change in gene expression of more than 2-fold as biologically relevant. Four genes (Fig. 6) were detected as biologically relevant and statistically significant (p>0.05): TNF receptor superfamily member 6 (Fas receptor; *FasR*), growth arrest-specific 6 (*Gas6*), tissue inhibitor of metalloproteinases 2 (*Timp2*), and vascular cell adhesion molecule-1 (*Vcam1*). In total, 10w and 20w CCR7$^{-/-}$ pMMCs produced 2.3 or 2.0-fold more *FasR* mRNA than the corresponding WT pMMCs (p=0.59 and 0.001, respectively). *Gas6* mRNA expression levels were reduced by a factor of 0.6 relative to 10w WT pMMCs (p=0.82) and 0.1 relative to 20w WT pMMCs (p=0.04). While there was no significant difference in *Timp2* expression between 10w pMMCs, 20w CCR7$^{-/-}$ pMMCs expressed 4.3 times more *Timp2* mRNA as opposed to 20w WT pMMCs (p=0.05). Compared with 10w WT pMMCs, a 3.2-fold increase of *Vcam1* mRNA expression was observed in 10w CCR7$^{-/-}$ pMMCs (p=0.01). Contrarily, in pMMCs from 20-weeks-old mice, the expression of *Vcam1* declined to 0.01-fold in CCR7$^{-/-}$ pMMCs relative to the WT (p=0.06).

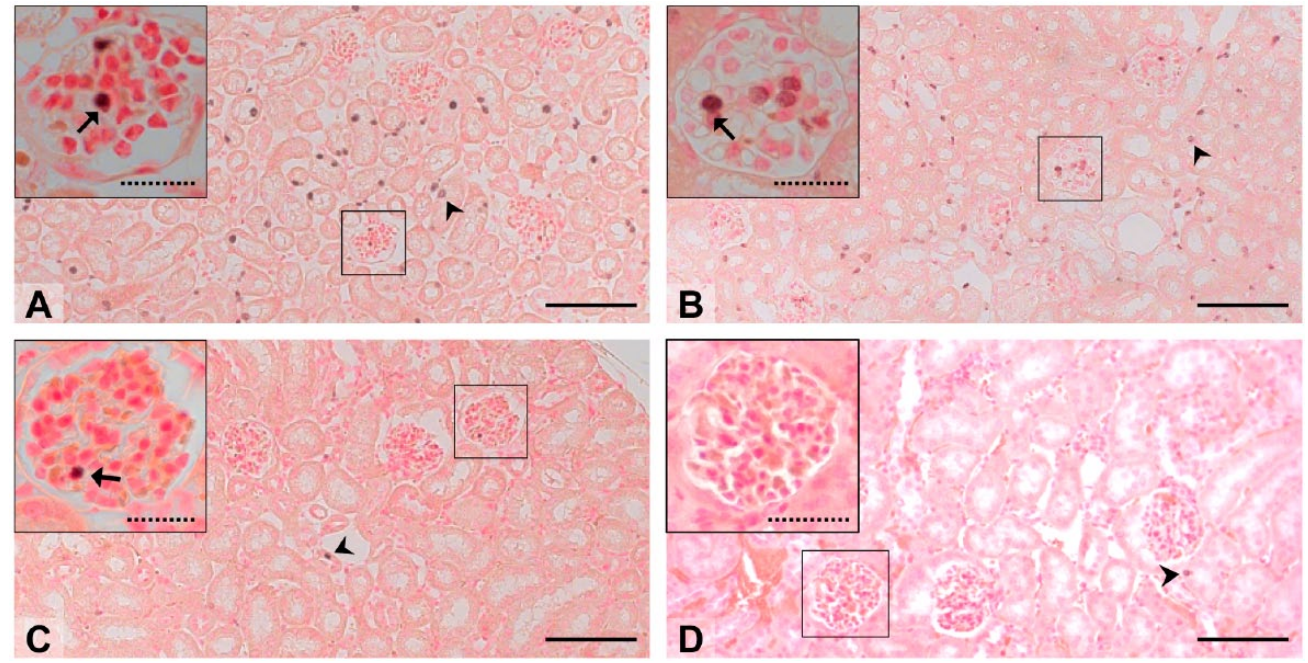

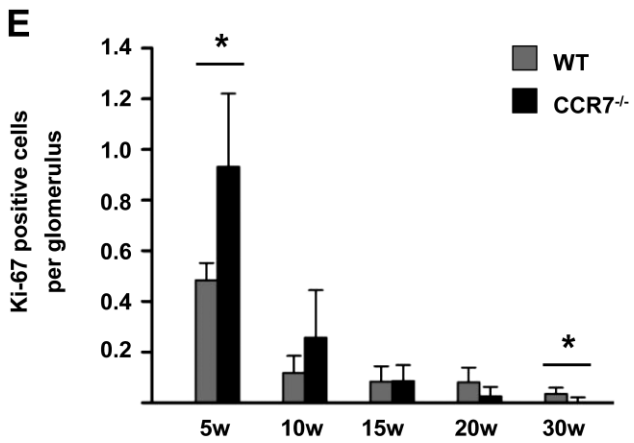

Figure 4. Renal and glomerular expression of Ki-67. (A–D) Renal specimens of 5-weeks-old (A) WT or (B) CCR7$^{-/-}$ and 30-weeks-old (C) WT or (D) CCR7$^{-/-}$ mice exhibit Ki-67 expressing cells stained in dark gray. Arrows indicate proliferating glomerular cells, arrow heads tubular cells. The marked areas in every overview are shown enlarged in the left corner. Scale bars: 100 µm, dashed scale bars: 25 µm. (E) Bars + *SD* represent the number of Ki-67 positive per glomerulus of 5-, 10-, 15-, 20-, and 30-weeks-old (w) WT (gray bar) and CCR7$^{-/-}$ (black bar) mice; 20 glomeruli per kidney were analyzed in a blinded manner. Abbreviation: WT, wild-type. *p<0.05; n=6–8.

CCR7 Deficiency Affected Proliferative Capability of pMMCs

Regarding the reduced number of glomerular MCs in CCR7$^{-/-}$ mice and the differential gene expression of *FasR* and *Gas6*, which regulate survival and proliferation, we studied the effect of CCR7 deficiency on the proliferative capability of pMMCs. We applied a 5-bromo-2′ deoxyuridine (BrdU) ELISA, which was conducted three times with pMMCs originating from a new passage each. The result (Fig. 7) was shown as mean absorption at 450 nm relative to 10w WT pMMCs. There is no difference between both WT pMMCs and 10w CCR7$^{-/-}$ pMMCs. Contrarily, 20w CCR7$^{-/-}$ pMMCs displayed a statistically significant reduced mean absorption, reflecting reduced proliferative properties.

Reduced Migratory Properties of CCR7 Deficient pMMCs

In addition to the BrdU ELISA, we performed a second experiment to confirm the relevance of CCR7 for mesangial proliferation but also coincidentally for mesangial migration. A wound-healing assay was conducted with pMMCs of each type. Cell migration was assessed immediately as well as 24 hr and 48 hr after the monolayer was injured (Fig. 8). Directly after wounding, a gap of circa 1.23 mm (±14 µm) was observed in all types of pMMCs. At 24 hr, WT pMMCs have already started to repopulate the vacant area and shortened the distance to 436 µm (±35 µm) or 523 µm (±130 µm) for cells from 10- or 20-weeks-old animals, respectively. In CCR7$^{-/-}$ pMMCs, this process took place decelerated, especially in 20w CCR7$^{-/-}$ pMMCs where we

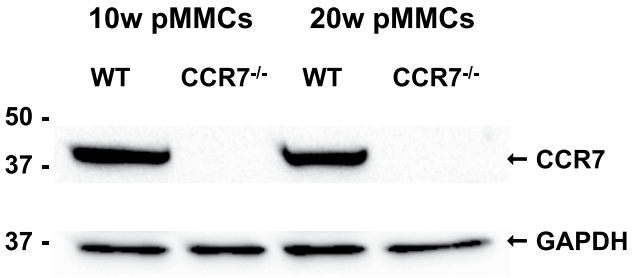

Figure 5. CCR7 protein expression by 10 and 20w WT and CCR7$^{-/-}$ pMMCs. Ten µg protein from the respective pMMC lysate was used for SDS-PAGE. Murine CCR7 has a molecular weight of 43 kDa, GAPDH of 36 kDa. Abbreviations: WT, wild-type; pMMCs, primary mouse mesangial cells; GAPDH, glyceraldehyde-3-phosphate dehydrogenase.

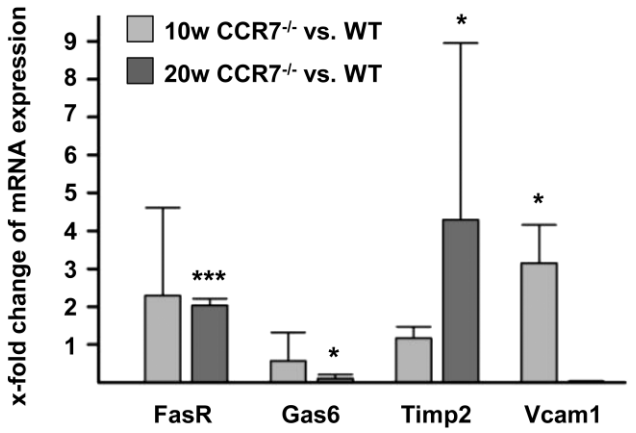

Figure 6. X-fold changes in mRNA expression of *FasR, Gas6, Timp2*, and *Vcam1*. The x-fold difference of the corresponding gene in CCR7$^{-/-}$ pMMCs relative to the age-matched WT pMMCs is represented by bars + *SD*. An x-fold change of 1 means no difference in mRNA expression level between the groups. RNA was extracted from all pMMC types, each from 3 different consecutive passages. Abbreviations: pMMCs, primary mouse mesangial cells; WT, wild-type. *p<0.05; ***p<0.001.

measured a wound of 1 mm (±303 µm) in the mean. After 48 hr, the lesion was almost completely closed in both WT pMMCs types, whereas a statistically significant wider gap of circa 472 µm (±78 µm) or 681 µm (±140 µm) was ascertained for 10w CCR7$^{-/-}$ pMMCs and 20w CCR7$^{-/-}$ pMMCs, respectively.

Induction of Renal CCR7 Expression in the Model of Anti-Thy1.1 Mesangioproliferative Glomerulonephritis

On one hand, CCR7 deficiency resulted in reduced mesangial cellularity in adult mice in vivo and impaired proliferative and migratory properties in

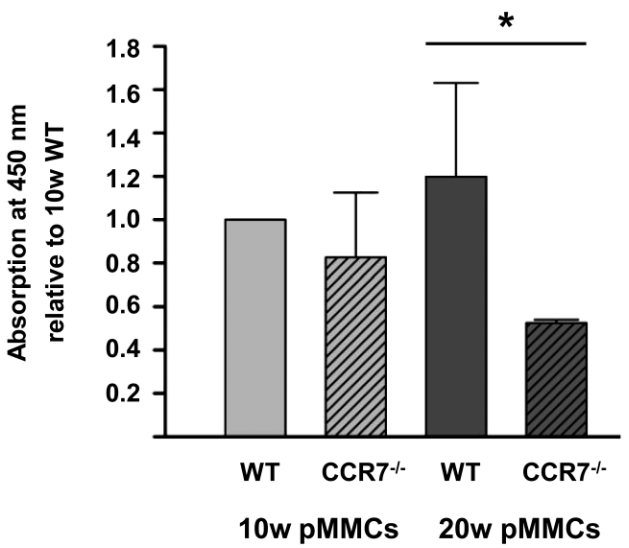

Figure 7. Proliferation assay. Bars + *SD* represent the mean absorption at 450 nm normalized to 10 WT pMMCs. The BrdU assay was conducted 3 times in three technical triplicate with 10 and 20w WT and CCR7$^{-/-}$ pMMCs, each from 3 different consecutive passages. Abbreviations: WT, wild-type; pMMCs, primary mouse mesangial cells; BrdU, bromo-2′ deoxyuridine. *p<0.05.

vitro. On the other hand, adult mice exhibited an only weak mesangial CCR7 expression. We wondered if this mesangial CCR7 expression could still play a role in adult animals under a disease condition. As such, we chose the induced Thy1.1 mesangioproliferative glomerulonephritis because like in nephrogenesis,[6] MCs have to migrate into the glomerulus, to proliferate, and to reorganize the capillary tuft.[23] Admittedly, this model exists only for rats not for mice but our localization experiment displays comparable results for untreated or PBS-treated WT mice and rats, respectively. Furthermore, it highlights the relevance of CCR7 as an important factor for mesangial physiology and repair.

As depicted in Fig. 9A–F, Thy1.1-specific OX 7 antibody injection induced mesangiolysis[24] followed by an extensive mesangial migration and proliferation.[23] This process correlated with the expression of the chemokine receptor. CCR7 was absent or weakly expressed in glomeruli of control rats treated with PBS (Fig. 9A), also see Supplemental Fig. 4. In contrast, a slight CCR7 expression was detected in the extraglomerular mesangium only 4 hr after antibody injection (Fig. 9B). However, 24 hr after OX-7 administration, the extraglomerular mesangium was considerably positive for CCR7 (Fig. 9C). Hereafter, the expression pattern changed from extraglomerular to intraglomerular between day 1 and 4 (Fig. 9D and E).

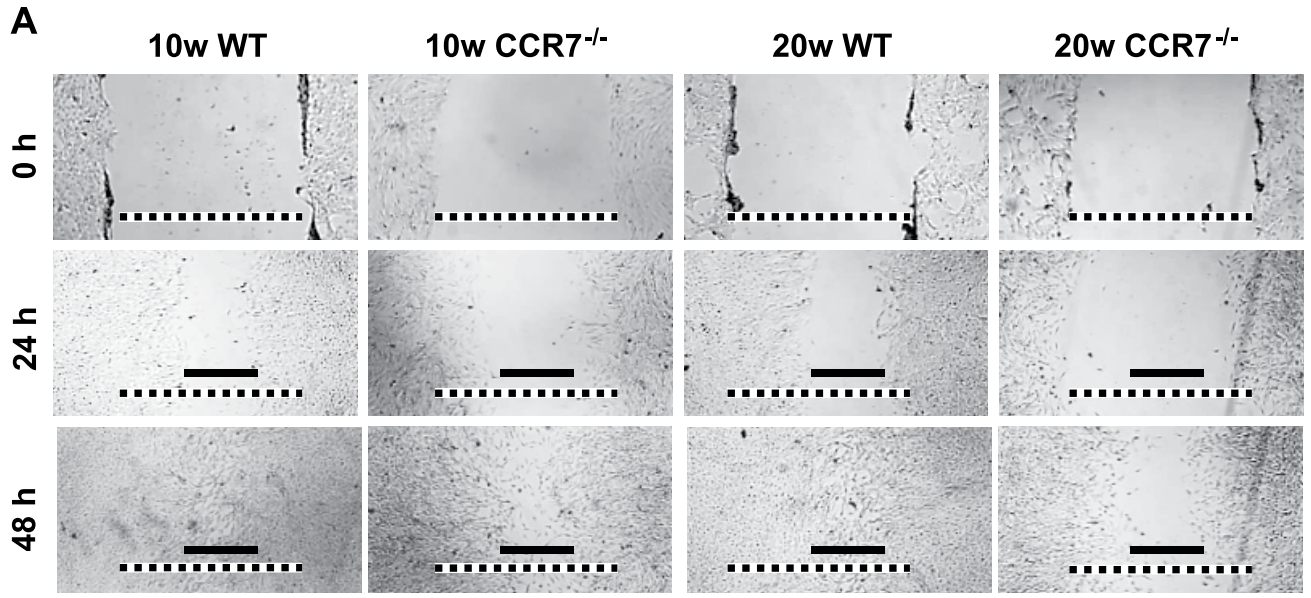

Figure 8. Cell migration assay. The pMMC layers from 10 and 20 weeks old WT and CCR7$^{-/-}$ mice were injured and the bridging of gap was documented by phase-contrast microscopy either immediately after wounding (0 hr; upper panel) as well as 1 (24 hr; middle panel) or 2 days (48 hr; lower panel) after wounding. Black scale bar: 0.5 mm; dashed scale bar: 1.25 mm. The reduced migratory properties of CCR7$^{-/-}$ pMMCs compared with WT pMMCs are also shown as graph with averaged values from 3 separate measurements (±*SD*). Abbreviations: pMMCs, primary mouse mesangial cells; WT, wild-type. *p<0.05 for CCR7$^{-/-}$ pMMCs compared with both WT pMMCs.

By the transition from extra- to intraglomerular CCR7 expression, the chemokine receptor initially localized mainly at the vascular pole of the glomerulus. Intraglomerular mesangial areas positive for CCR7 expanded in the progression of experimental glomerulonephritis while the extraglomerular expression of the molecule disappeared. At day 7 (Fig. 9F) after OX-7 administration, CCR7 ceased to be expressed in most glomeruli.

These results could be further supported by mRNA expression analysis. On the transcriptional level, we detected a maximum expression of CCR7 at day 2. Afterward, CCR7 mRNA declined again, and interestingly, the mRNA expression of CCL21 followed an analogous course (Suppl. Table 3). Furthermore, we wanted to exclude that CCR7-positive staining could be caused by infiltrating immune cells. Using sequential sections, an IHC localization of CCR7, CD68, a marker for macrophages, and CD3, a pan T-cell marker, was conducted. In nearly all sections, the expression pattern of the chemokine receptor did not coincide with CD68 or CD3 (Supplemental Fig. 4).

Discussion

The aim of this study was to reveal the expanded function of CCR7 in mesangial physiology. The activation of the chemokine receptor induces and enhances not only leukocyte migration[8–10] but also MC proliferation, migration, and repair. Our localization experiments clearly showed that CCR7 and CCL21 were expressed in spatial proximity during glomerulogenesis. Direct cell-to-cell signaling between intrinsic glomerular cells is known to be important to both glomerular homeostasis and responses to local injury.[25,26] In addition to this ligand-receptor pair, the expression of various CXC-chemokines has already been described in human[27] and rodent[28] nephrogenesis. Whereas the physiological relevance of CXC-chemokines is associated with their proangiogenic properties,[29,30] a deficiency of the

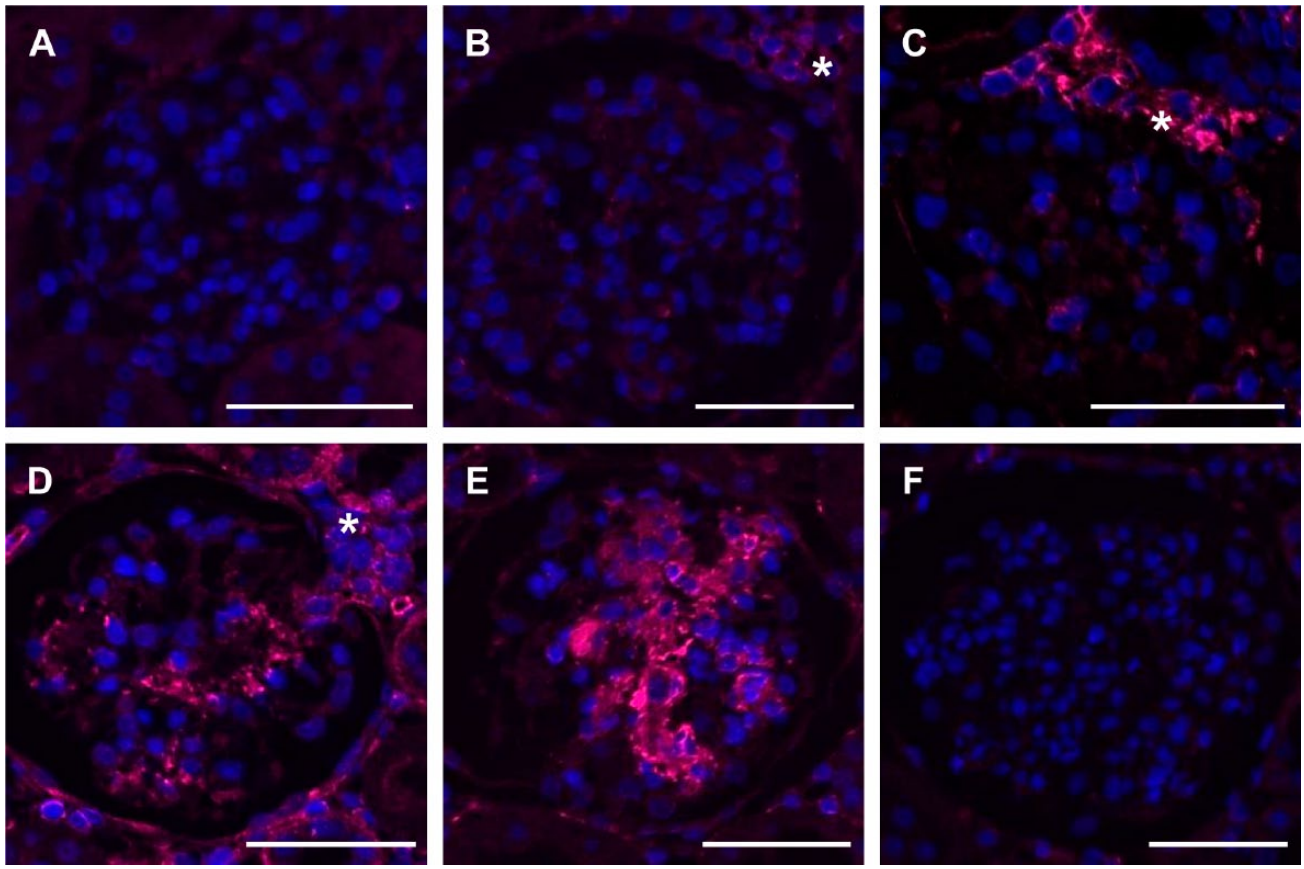

Figure 9. Fluorescent IHC detection of CCR7 in rats after induction of anti-Thy1.1 mesangioproliferative glomerulonephritis. (A) No glomerular CCR7 staining is visible in PBS-treated control rat. (B) 4 hr after application of the anti-Thy1.1 antibody, a weak CCR7 expression (magenta) is recognizable within the extraglomerular mesangium (*). (C) The CCR7 expression becomes more pronounced after 24 hr. (D) After 48 hr, the extra- and intraglomerular mesangium are CCR7-positive. (E) Shows a mesangial expression pattern at day 4. (F) 7 days after mesangiolysis was induced, CCR7 cannot be detected in glomeruli anymore. Scale bars: 100 μm; *n*=4.

receptor CXCR4[31] is perinatally lethal. CCR7 and CCL21, however, represent the first CC-chemokine ligand-receptor pair to be expressed by renal non-immune cells under physiological conditions. In developing glomeruli, CCR7 exhibited a mesangial expression pattern while CCL21 localized on podocytes, which allows an efficient CCR7-mediated MC stimulation by adjacent podocytes.

PDGFR-β represents the key molecule for mesangial migration and so for glomerular development. Mice deficient in PDGFR-β display aneurysmatic glomeruli without immigrated MC.[32,33] Contrarily to PDGFR-β, mesangial migration and capillary tuft formation also occurred in the absence of CCR7, however, chemokine receptor signaling promoted both processes. Our study gives evidence that mesangial migration and tuft formation markedly benefits from CCR7 and CCL21 expression during nephrogenesis whereas other aspects of renal development were not influenced by CCR7 deficiency. So, we could not detect any differences in the width of the nephrogenic zone or the number of glomeruli. Previous in vitro analyses revealed that stimulation with CCL21 results in an enhanced ability of MCs to reorganize their cytoskeleton[17,18] by causing increased membrane ruffling and formation of filamentous cell extensions establishing connections to neighboring cells.[17] This heightened ability may have a positive effect on capillary tuft formation because changes in the organization of the cytoskeleton and the competence to establish contact to other cells and structures serve as essential requirements to bind to laminin α5 in the GBM in glomerulogenesis.[6] As a consequence at pp10, significantly more CLS bodies were observed in CCR7$^{-/-}$ mice. Even 5-weeks-old CCR7$^{-/-}$ mice featured more glomeruli with a reduced MC number and an imperfect convoluted tuft. To compensate this developmental deficit, animals needed to reach the age of 10 weeks. CCR7 deficiency, however, not only affected mesangial cellularity during the renal development but also in adult animals. Twenty- and

30-week-old CCR7$^{-/-}$ mice exhibited significantly less MCs than the age-matched WT pendant. Our findings clearly demonstrate that MCs respond to CCR7-CCL21 signaling both during nephrogenesis and in adult mice to maintain MC function and physiology. In addition, this role of the chemokine receptor-ligand-pair is specific for MCs.

At the age of 5 weeks, there were more proliferating cells in CCR7$^{-/-}$ mice than in the WT pendant. This matches with the observation that mesangial fields and glomerular tufts were not fully developed at this age. Consistently, there was a necessity that CCR7$^{-/-}$ mesangial cells proliferate differently to regain the developmental deficit. Later, at the age of 30 weeks, the opposite was the case. In glomeruli of the oldest CCR7$^{-/-}$ mice, proliferating cells were observed very rarely, whereas in age-matched WT animals, still cells proliferated. This result is in accordance with the reduced amount of glomerular MCs in 30-weeks-old CCR7$^{-/-}$ mice. In contrast, Ki-67 positive tubule cells were detected in both 30-weeks-old WT and CCR7$^{-/-}$ mice. This supports our hypothesis that CCR7 plays an important role specifically in MCs.

Additional in vitro experiments confirmed the physiological relevance of the chemokine receptor CCR7. Ten and 20w WT pMMCs expressed high levels of CCR7 protein although both the cellular mRNA expression level and the in vivo CCR7 protein expression were very low. According to Schaeble et al., CCR7 is ubiquitylated in a constitutive and ligand-independent manner.[34] This results in an efficient recycling of the receptor and prevents degradation. Moreover, Johno and Kitamura[35] reported that MCs in vivo under healthy conditions are quiescent. In this physiological state, they do not express α-smooth muscle actin (α-SMA), a marker often described to stain for activated MCs during experimental diseases. In mesangioproliferative glomerulonephritis (e.g., Thy1.1 glomerulonephritis), however, MCs not only express α-SMA but also show proliferation and migration. Cultured MCs represent a non-quiescent state that is associated with α-SMA expression, proliferation, and migration. Our studies suggest that CCR7 also plays a role in proliferation and migration because CCR7$^{-/-}$ pMMCs displayed restricted capabilities regarding in vitro wound-healing experiments. This was further supported by differential mRNA expression of various genes dependent on the genotype (see below). Consequently, the chemokine receptor serves as proliferation and survival factor for MC in vivo and in vitro.

To show the decreased proliferative and migratory capabilities of CCR7$^{-/-}$ pMMCs, we performed 2 in vitro experiments: a BrdU ELISA and a wound-healing assay. Both give evidence that the mere absence of CCR7 negatively influences these properties. CCR7$^{-/-}$ pMMCs expressed more *FasR* mRNA and less *Gas6* mRNA than WT pMMCs. FASR induces apoptosis.[36] Whereas several research groups demonstrated induction of MC death via FASR,[37,38] we previously showed that stimulation of human MCs with CCL21 resulted in a reduced susceptibility to FAS antibody induced apoptosis.[15] This indicates that CCR7$^{-/-}$ pMMCs were less protected from cell death in vitro. Furthermore, this correlates with our in vivo data that unveiled a decline in MC number in 20-weeks-old CCR7$^{-/-}$ mice. The impaired mesangial physiology could also refer to the decreased mRNA expression of *Gas6*. This molecule mediates the activation of several downstream signal cascades including proliferation, migration, and survival of many cell types.[39] GAS6 also serves as autocrine growth factor for MCs.[40,41] Therefore, our analysis indicates that especially 20w CCR7$^{-/-}$ pMMCs received considerably less activation signals due to reduced expression of *Gas6*.

Another two differentially expressed genes, *Timp2* and *Vcam1*, are associated with cell migration. TIMP2 acts as an inhibitor of matrix metalloproteinase 2, which for its part promotes mesangial proliferation[42] and migration.[43] Despite contrasting publications regarding the effect of TIMP2 on cell migration,[44,45] we conclude that the elevated *Timp2* expression in 20w CCR7$^{-/-}$ pMMCs correlates with the reduced migratory properties of CCR7$^{-/-}$ pMMCs regarding our wound-healing assay. VCAM1 is important for directional cell motion, especially for leukocytes[46,47] but it was also ascertained in cultured MCs.[48,49] We suppose that changes in *Vcam1* mRNA expression may contribute to explain the impaired migratory properties of CCR7$^{-/-}$ pMMCs.

The spatiotemporally regulated chemokine receptor expression in rats after induction of anti-Thy1.1 mesangioproliferative glomerulonephritis gives further evidence for the expanded role of CCR7 in mesangial physiology. The Thy1.1 glomerulonephritis proceeded as described previously by others.[23,50] Control rats treated with PBS exhibited very weak mesangial CCR7 expression. This result is analogous to the low mesangial CCR7 expression in adult mice. After induction of mesangiolysis, however, cells in the extraglomerular mesangium started to re-express the receptor. Later cells apparently migrating into the glomerulus and proliferating in there were positive for CCR7. Because CCR7 could not be localized after the migration and proliferation process was completed, our study suggests that CCR7 is important for directing of MC migration and promoting their expansion in a spatiotemporally limited manner.

Additional analyses are required to further elucidate the role of CCR7 in mesangioproliferative glomerulonephritis. Nevertheless, comparison between CCR7 expression sites and duration in nephrogenesis and after induction of mesangiolysis shows one similarity. The chemokine receptor is expressed by (early) MCs until their migration and proliferation phase has terminated. Or, in other words and with respect to our analysis of the mesangial cellularity in WT and CCR7$^{-/-}$ mice, the BrdU ELISA, and wound-healing assay, only MCs that express CCR7 are able to proliferate and migrate in an efficient manner.

In conclusion, our studies show that CCR7 serves as an important factor for mesangial migration, proliferation, and repair. Therefore, this chemokine receptor plays a pivotal role in MC physiology both in vivo and in vitro.

Acknowledgments

We thank Ms. Kathrin Eidenschink, Ms. Alexandra Mueller, and Ms. Brigitte Ruhland for their excellent technical assistance. This work was supported by the Deutsche Forschungsgemeinschaft (SFB699).

Competing Interests

The author(s) declared no potential conflicts of interest with respect to the research, authorship, and/or publication of this article.

Author Contributions

BB and AK designed and headed the study. SW wrote the manuscript. SW conducted the IHC staining, single cell analysis, immunoblotting, qPCR analyses, and cell culture experiments. EMRJ performed pMMC isolation and cell culture experiments. CRR conducted the Thy1.1 study. AS and MCB collaborated in realization and analysis of the study.

Funding

The author(s) disclosed receipt of the following financial support for the research, authorship, and/or publication of this article: This work as sub-project B10 of SFB699 (speaker: Prof. A.K.) was supported in parts by the "Deutsche Forschungsgemeinschaft."

Literature Cited

1. Grobstein C. Inductive tissue interaction in development. Adv Cancer Res. 1956;4:187–236.
2. Grobstein C. Inductive epitheliomesenchymal interaction in cultured organ rudiments of the mouse. Science. 1953;118:52–5.
3. Saxén L. Organogenesis of the Kidney. Cambridge, United Kingdom: Cambridge University Press; 1987.
4. Ekblom P, Sariola H, Karkinen-Jaaskelainen M, Saxen L. The origin of the glomerular endothelium. Cell Differ. 1982;11:35–9.
5. Ricono JM, Xu YC, Arar M, Jin DC, Barnes JL, Abboud HE. Morphological insights into the origin of glomerular endothelial and mesangial cells and their precursors. J Histochem Cytochem. 2003;51:141–50.
6. Kikkawa Y, Virtanen I, Miner JH. Mesangial cells organize the glomerular capillaries by adhering to the G domain of laminin alpha5 in the glomerular basement membrane. J Cell Biol. 2003;161:187–96.
7. Rossi D, Zlotnik A. The biology of chemokines and their receptors. Annu Rev Immunol. 2000;18:217–42.
8. Nagira M, Imai T, Yoshida R, Takagi S, Iwasaki M, Baba M, Tabira Y, Akagi J, Nomiyama H, Yoshie O. A lymphocyte-specific CC chemokine, secondary lymphoid tissue chemokine (SLC), is a highly efficient chemoattractant for B cells and activated T cells. Eur J Immunol. 1998;28:1516–23.
9. Sallusto F, Schaerli P, Loetscher P, Schaniel C, Lenig D, Mackay CR, Qin S, Lanzavecchia A. Rapid and coordinated switch in chemokine receptor expression during dendritic cell maturation. Eur J Immunol. 1998;28: 2760–9.
10. Forster R, Schubel A, Breitfeld D, Kremmer E, Renner-Muller I, Wolf E, Lipp M. CCR7 coordinates the primary immune response by establishing functional microenvironments in secondary lymphoid organs. Cell. 1999;99:23–33.
11. Strieter RM, Polverini PJ, Kunkel SL, Arenberg DA, Burdick MD, Kasper J, Dzuiba J, Van DJ, Walz A, Marriott D. The functional role of the ELR motif in CXC chemokine-mediated angiogenesis. J Biol Chem. 1995;270:27348–57.
12. Strieter RM, Kunkel SL, Elner VM, Martonyi CL, Koch AE, Polverini PJ, Elner SG. Interleukin-8. A corneal factor that induces neovascularization. Am J Pathol. 1992;141:1279–84.
13. Prodjosudjadi W, Gerritsma JS, Klar-Mohamad N, Gerritsen AF, Bruijn JA, Daha MR, van Es LA. Production and cytokine-mediated regulation of monocyte chemoattractant protein-1 by human proximal tubular epithelial cells. Kidney Int. 1995;48:1477–86.
14. Romagnani P, Beltrame C, Annunziato F, Lasagni L, Luconi M, Galli G, Cosmi L, Maggi E, Salvadori M, Pupilli C, Serio M. Role for interactions between IP-10/Mig and CXCR3 in proliferative glomerulonephritis. J Am Soc Nephrol. 1999;10:2518–26.
15. Banas B, Wornle M, Berger T, Nelson PJ, Cohen CD, Kretzler M, Pfirstinger J, Mack M, Lipp M, Grone HJ, Schlondorff D. Roles of SLC/CCL21 and CCR7 in human kidney for mesangial proliferation, migration, apoptosis, and tissue homeostasis. J Immunol. 2002;168:4301–7.
16. Banas B, Luckow B, Moller M, Klier C, Nelson PJ, Schadde E, Brigl M, Halevy D, Holthofer H, Reinhart B, Schlondorff D. Chemokine and chemokine receptor expression in a novel human mesangial cell line. J Am Soc Nephrol. 1999;10:2314–22.

17. Banas B, Wornle M, Merkle M, Gonzalez-Rubio M, Schmid H, Kretzler M, Pietrzyk MC, Fink M, Perez de LG, Schlondorff D. Binding of the chemokine SLC/CCL21 to its receptor CCR7 increases adhesive properties of human mesangial cells. Kidney Int. 2004;66:2256–63.
18. Wornle M, Schmid H, Merkle M, Banas B. Effects of chemokines on proliferation and apoptosis of human mesangial cells. BMC Nephrol. 2004;5:8.
19. Popescu CR, Sutherland MR, Cloutier A, Benoît G, Bertagnolli M, Yzydorczyk C, Germain N, Phan V, Lelievre-Pegorier M, Sartelet H, Nuyt AM. Hyperoxia exposure impairs nephrogenesis in the neonatal rat: role of HIF-1α. PLoS ONE. 2013;8:e82421.
20. Ecker RC, Steiner GE. Microscopy-based multicolor tissue cytometry at the single-cell level. Cytometry A. 2004;59:182–90.
21. Alpers CE, Seifert RA, Hudkins KL, Johnson RJ, Bowen-Pope DF. PDGF-receptor localizes to mesangial, parietal epithelial, and interstitial cells in human and primate kidneys. Kidney Int. 1993;43:286–94.
22. Seifert RA, Alpers CE, Bowen-Pope DF. Expression of platelet-derived growth factor and its receptors in the developing and adult mouse kidney. Kidney Int. 1998;54:731–46.
23. Hugo C, Shankland SJ, Bowen-Pope DF, Couser WG, Johnson RJ. Extraglomerular origin of the mesangial cell after injury. A new role of the juxtaglomerular apparatus. J Clin Invest. 1997;100:786–94.
24. Morita T, Churg J. Mesangiolysis. Kidney Int.1983;24:1–9.
25. Schlöndorff D, Banas B. The mesangial cell revisited: no cell is an island. J Am Soc Nephrol. 2009;6:1179–87.
26. Sison K, Eremina V, Baelde H, Min W, Hirashima M, Fantus IG, Quaggin SE. Glomerular structure and function require paracrine, not autocrine, VEGF-VEGFR-2 signaling. J Am Soc Nephrol. 2010;21:1691–701.
27. Grone HJ, Cohen CD, Grone E, Schmidt C, Kretzler M, Schlondorff D, Nelson PJ. Spatial and temporally restricted expression of chemokines and chemokine receptors in the developing human kidney. J Am Soc Nephrol. 2002;13:957–67.
28. Levashova ZB, Sharma N, Timofeeva OA, Dome JS, Perantoni AO. ELR+-CXC chemokines and their receptors in early metanephric development. J Am Soc Nephrol. 2007;18:2359–70.
29. Backer MV, Levashova Z, Patel V, Jehning BT, Claffey K, Blankenberg FG, Backer JM. Molecular imaging of VEGF receptors in angiogenic vasculature with single-chain VEGF-based probes. Nat Med. 2007;13:504–9.
30. Strieter RM, Polverini PJ, Kunkel SL, Arenberg DA, Burdick MD, Kasper J, Dzuiba J, Van DJ, Walz A, Marriott D. The functional role of the ELR motif in CXC chemokine-mediated angiogenesis. J Biol Chem. 1995;270:27348–57.
31. Takabatake Y, Sugiyama T, Kohara H, Matsusaka T, Kurihara H, Koni PA, Nagasawa Y, Hamano T, Matsui I, Kawada N, Imai E, Nagasawa T, Rakugi H, Isaka Y. The CXCL12 (SDF-1)/CXCR4 axis is essential for the development of renal vasculature. J Am Soc Nephrol. 2009;20:1714–23.
32. Leveen P, Pekny M, Gebre-Medhin S, Swolin B, Larsson E, Betsholtz C. Mice deficient for PDGF B show renal, cardiovascular, and hematological abnormalities. Genes Dev. 1994;8:1875–87.
33. Soriano P. Abnormal kidney development and hematological disorders in PDGF beta-receptor mutant mice. Genes Dev. 1994;8:1888–96.
34. Schaeuble K, Hauser MA, Rippl AV, Bruderer R, Otero C, Groettrup M, Legler DF. Ubiquitylation of the chemokine receptor CCR7 enables efficient receptor recycling and cell migration. J Cell Sci. 2012;125:4463–74.
35. Johno H, Kitamura M. Pathological in situ reprogramming of somatic cells by the unfolded protein response. Am J Pathol. 2013;183:644–54.
36. Nagata S, Golstein P. The Fas death factor. Science. 1995;267:1449–56.
37. Gonzalez-Cuadrado S, Lopez-Armada MJ, Gomez-Guerrero C, Subira D, Garcia-Sahuquillo A, Ortiz-Gonzalez A, Neilson EG, Egido J, Ortiz A. Anti-Fas antibodies induce cytolysis and apoptosis in cultured human mesangial cells. Kidney Int. 1996;49:1064–70.
38. Huang Y, Luo F, Li H, Jiang T, Zhang N. Conditioned medium from alternatively activated macrophages induce mesangial cell apoptosis via the effect of Fas. Exp Cell Res. 2013;319:3051–7.
39. Axelrod H, Pienta KJ. Axl as a mediator of cellular growth and survival. Oncotarget. 2014;5:8818–52.
40. Yanagita M, Arai H, Nakano T, Ohashi K, Mizuno K, Fukatsu A, Doi T, Kita T. Gas6 induces mesangial cell proliferation via latent transcription factor STAT3. J Biol Chem. 2001;276:42364–9.
41. Yanagita M, Ishii K, Ozaki H, Arai H, Nakano T, Ohashi K, Mizuno K, Kita T, Doi T. Mechanism of inhibitory effect of warfarin on mesangial cell proliferation. J Am Soc Nephrol. 1999;10:2503–9.
42. Turck J, Pollock AS, Lee LK, Marti HP, Lovett DH. Matrix metalloproteinase 2 (gelatinase A) regulates glomerular mesangial cell proliferation and differentiation. J Biol Chem. 1996;271:15074–83.
43. Wang Y, Li M, Xu Y, He N, Leng L, Li Z. Tumor necrosis factor-α regulates matrix metalloproteinase-2 expression and cell migration via ERK pathway in rat glomerular mesangial cells. Cell Biol Int. 2014;38:1060–8.
44. Ahn SM, Jeong SJ, Kim YS, Sohn Y, Moon A. Retroviral delivery of TIMP-2 inhibits H-ras-induced migration and invasion in MCF10A human breast epithelial cells. Cancer Lett. 2004;207:49–57.
45. Terasaki K, Kanzaki T, Aoki T, Iwata K, Saiki I. Effects of recombinant human tissue inhibitor of metalloproteinases-2 (rh-TIMP-2) on migration of epidermal keratinocytes in vitro and wound healing in vivo. J Dermatol. 2003;30:165–72.
46. Osborn L, Hession C, Tizard R, Vassallo C, Luhowskyj S, Chi-Rosso G, Lobb R. Direct expression cloning of vascular cell adhesion molecule 1, a cytokine-induced

endothelial protein that binds to lymphocytes. Cell. 1989;59:1203–11.
47. Carlos TM, Schwartz BR, Kovach NL, Yee E, Rosa M, Osborn L, Chi-Rosso G, Newman B, Lobb R. Vascular cell adhesion molecule-1 mediates lymphocyte adherence to cytokine-activated cultured human endothelial cells. Blood. 1990;76:965–70.
48. Wuthrich RP. Cell adhesion molecules and inflammatory renal diseases. Nephrol Dial Transplant. 1994;9:1063–5.
49. Lee IT, Shih RH, Lin CC, Chen JT, Yang CM. Role of TLR4/NADPH oxidase/ROS-activated p38 MAPK in VCAM-1 expression induced by lipopolysaccharide in human renal mesangial cells. Cell Commun Signal. 2012;10:33.
50. Chen D, Li Y, Mei Y, Geng W, Yang J, Hong Q, Feng Z, Cai G, Zhu H, Shi S, Bai XY, Chen X. miR-34a regulates mesangial cell proliferation via the PDGFR-β/Ras-MAPK signaling pathway. Cell Mol Life Sci. 2014;71:4027–42.